JOURNAL OF MATERIALS SCIENCE 19 (1984) 1476–1485

SAXS study on crystallization of an amorphous $Pd_{76}Au_6Si_{18}$ alloy

RYOSUKE O. SUZUKI, KOZO OSAMURA
School of Metallurgy and Materials Science, Kyoto University, Sakyo-ku, Kyoto 606, Japan

The crystallization behaviour of an amorphous $Pd_{76}Au_6Si_{18}$ alloy has been investigated mainly by means of small angle X-ray scattering measurements. The amorphous alloy crystallized to form MS-I phase with composition $Pd_{78}Au_{22}$ in the amorphous matrix, which later crystallized as MS-II. The crystallization kinetics of MS-I phase were analysed in the framework of conventional nucleation theory. It was suggested that the considerable number of nuclei of MS-I phase had been already formed in the as-quenched specimen and the remaining nucleation attained within the short period of isothermal ageing. The remarkable increase of the scattering intensity corresponded to the growth of MS-I phase, the kinetics of which were found to be controlled by the diffusion mechanism. The interdiffusion constant was obtained from $D = 6.0 \times 10^{15} \exp(-420\,\text{kJ mol}^{-1}/RT)\ \text{m}^2\ \text{sec}^{-1}$, which agreed fairly with the reported values.

1. Introduction

Amorphous Pd–Si alloy has become one of the well known amorphous materials since the report by Duwez *et al.* [1]. The amorphous alloy can be prepared by rapidly quenching in the concentration range from 16 to 22 at% silicon [2]. The study of the crystallization reactions has been performed by many authors [3–8]. Masumoto *et al.* [3] reported that the metastable crystalline phase with fcc structure, which is called MS-I, appeared firstly in the amorphous phase by the heat treatment at relatively high temperature and consequently the second metastable phase called MS-II with orthorhombic symmetry crystallized. Recently other phases, such as Pd_9Si_2, Pd_5Si and Pd_3Si, have been reported to crystallize from the amorphous phase [5, 6, 9]. There are several studies on the crystallization of ternary Pd–Si amorphous alloys with copper [10–12], silver [10, 13], gold [10, 14], iron [15, 16], nickel [17] and antimony [18].

Among these investigations, the kinetics of crystallization have been mainly analysed in terms of Johnson–Mehl–Avrami's equation from the change of physical properties. However, the kinetics exponents obtained experimentally seem to vary among authors, depending on the alloy system and its thermal history [8, 11, 13, 14]. Chou and Turnbull [14] obtained the following results in the Pd–Au–Si ternary system. The $Pd_{74}Au_8Si_{18}$ amorphous alloy phase-separated initially to two supercooled liquids above the glass transition temperature (T_g), each of which later crystallized in turn. On the other hand, the $Pd_{80}Au_{3.5}Si_{16.5}$ amorphous alloy phase-separated to form a fcc phase dispersed in the amorphous phase, which later crystallized. Our recent study [19] made clear that the amorphous $Pd_{82-x}Au_xSi_{18}$ ($x = 0$ to 8) alloy relaxed in structure prior to the crystallization, when the specimen was isothermally held at a temperature below T_g, and the relaxed structure turned back reversibly to the supercooled liquid by a short time re-heating at the temperature above T_g.

In the present study, the crystallization kinetics for an amorphous $Pd_{76}Au_6Si_{18}$ alloy have been investigated in conjunction with the structural relaxation mainly by means of small angle X-ray scattering (SAXS) measurements as well as by transmission electron microscopic (TEM) observation.

0022–2461/84 $03.00 + .12

2. Experimental methods

High purity palladium, gold and silicon were weighed to the nominal composition with $Pd_{82-x}Au_xSi_{18}$ in at% ($x = 0$, 2, 4, 6 and 8) and melted in an evacuated quartz tube. The amorphous ribbons were prepared in a form of ribbons about 20 μm thick and 5 mm wide by using the single roller technique. In the present study, the $Pd_{76}Au_6Si_{18}$ alloy was mainly investigated. The specimens were heat-treated in the evacuated fused quartz tube by using the salt bath regulated within 0.5 K.

SAXS measurements were performed by the MoK_α characteristic X-ray and by using a Kratky type U-slit. The details of the intensity analysis have been reported previously [20]. In order to check the structural change during the heat treatment, the diffraction intensity was measured over the wide range of scattering angles by the θ-2θ diffractometer in transmission geometry. For the determination of the lattice constant, an extrapolation function reported by Nelson and Riley [21] was adopted. The specimen for TEM observation was prepared by electropolishing using the electrolyte with 23 vol% perchloric acid and 77 vol% acetic acid. The thinned specimens were examined in a JEM-120 transmission electron microscope.

3. Experimental results

As reported previously [19], $Pd_{76}Au_6Si_{18}$ amorphous alloy crystallized after structural relaxation during isothermal ageing at temperatures below T_g, which was 655 K for the present alloy. Diffraction measurements made clear that the first crystallized phase has fcc structure and that its lattice constant is 0.3936 ± 0.0006 nm. This phase is consistent with the MS-I phase reported by the other authors [3]. Its value was larger than the lattice constant of 0.3890 ± 0.0002 nm for pure palladium and also larger than the value of 0.3905 ± 0.0001 nm for the $Pd_{76}Au_6$ solid solution fully annealed. This fact suggested that the composition of the MS-I phase should be enriched by the third element, that is, gold. When the alloy aged at temperatures between 633 and 653 K, the lattice constant of its MS-I phase did not change within experimental error.

In order to examine the composition dependence of the lattice constant of the MS-I phase, the measurement was performed for $Pd_{82-x}Au_xSi_{18}$ alloys aged at 723 K for 900 sec. The result is shown in Fig. 1. The lattice constant increased linearly with increasing gold content. As shown also in Fig. 1, the lattice constant for Pd–Au solid solution was reported to increase with increasing gold content [22]. The solubility of silicon in palladium is known to be negligibly small in the crystalline equilibrium state [23]. Here, therefore, it was assumed that the content of silicon in the MS-I phase crystallized from the $Pd_{82-x}Au_xSi_{18}$ amorphous alloy was neglected and the amount of the increase of lattice constant due to gold content was equivalent to the case in the Pd–Au binary crystalline system. Consequently, the chemical form of the MS-I phase in the $Pd_{76}Au_6Si_{18}$ alloy was evaluated to be $Pd_{78}Au_{22}$.

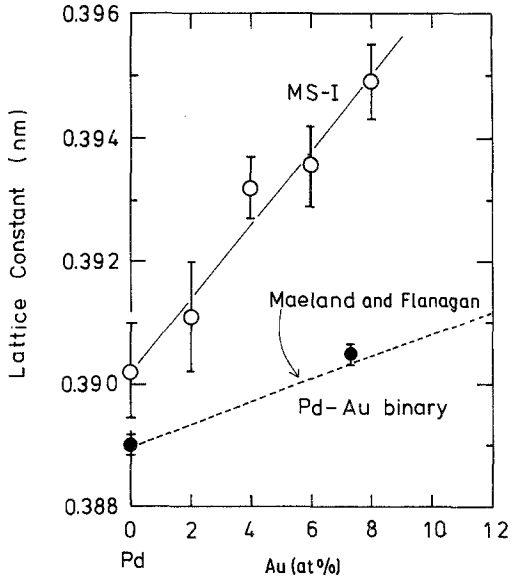

Figure 1 Lattice constant of the MS-I phase crystallized from the amorphous $Pd_{82-x}Au_xSi_{18}$ alloys (open circles) and that of well annealed pure palladium and $Pd_{76}Au_6$ (closed circles), where the dashed line indicates the lattice constant for binary Pd–Au alloy after Maeland and Flanagan [22].

After the crystallization of the MS-I phase, another crystalline phase showing complicated diffraction patterns appeared. Its structure could be assigned to have orthrhombic symmetry with lattice constants $a = 0.575 \pm 0.001$ nm, $b = 0.755 \pm 0.002$ nm and $c = 0.525 \pm 0.001$ nm, respectively, which was consistent with the reported values of Pd_3Si [24]. Considering the sequence of the crystallization process, this phase should correspond to MS-II as proposed by Masumoto *et al.* [3].

Fig. 2 shows the result of TEM observation for

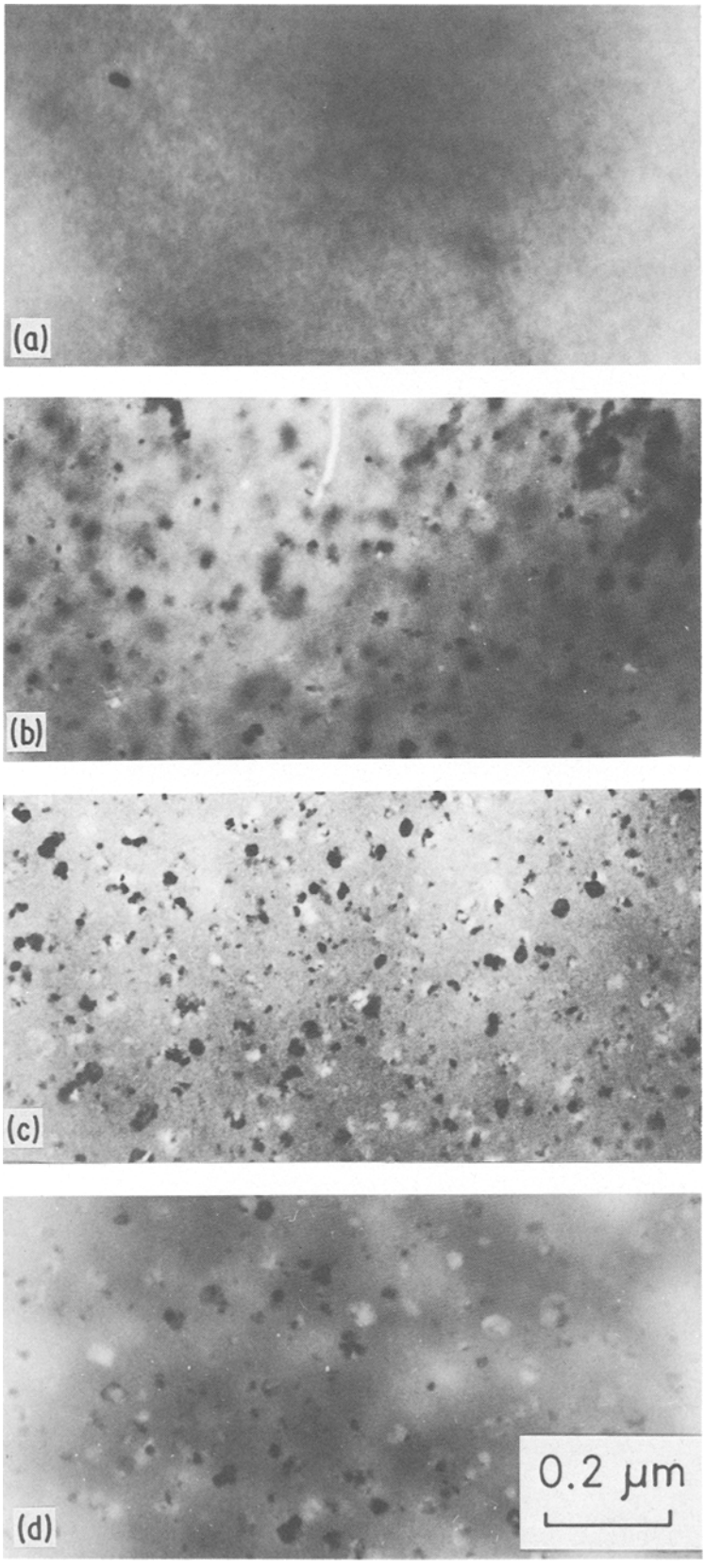

Figure 2 Change in structure of the amorphous $Pd_{76}Au_6Si_{18}$ alloy aged at 638 K for (a) 12 ksec, (b) 24 ksec, (c) 42 ksec and (d) 60 ksec.

the $Pd_{76}Au_6Si_{18}$ amorphous alloy aged at 638 K. Even after the 12 ksec ageing, a small amount of very fine particles was observed in some places of the amorphous matrix. The longer the ageing time, the larger the size of crystalline particles. Their shape was recognized to be nearly spherical as seen in the specimen aged for 24 ksec. The selected area diffraction patterns for the MS-I phase, as mentioned in the above paragraph, were firstly detected for the specimen aged for 24 ksec. The shape of each particle changed irregularly with increasing size as seen in the specimen aged for 60 ksec. After the crystallization of the MS-II phase, the specimen became so brittle that the TEM observation could not be done.

As mentioned previously [25], the observed SAXS intensity consists of several kinds of scattering sources, that is, the coherent scattering, $J_{coh}(s)$, the fluorescence excited by Mo$K\alpha$ radiation, $J_{fl}(s)$, and the parasitic scattering, $J_{BG}(s)$. The counting rate, $E(s)$, at a scattering vector, s ($4\pi \sin\theta/\lambda$), normalized by that from the standard materials, E_0, could be expressed by the equation,

$$E(s)/E_0 = tT[J_{coh}(s) + J_{fl}(s)] + TJ_{BG}(s) \quad (1)$$

where t is the sample thickness and T is the transmission. After the partial correction, the term, $J_{coh}(s) + J_{fl}(s)$ was obtained as shown in Fig. 3. When the specimen was aged at 638 K, the SAXS intensity increased with increasing ageing time. Comparing with the TEM observation, the increase of SAXS intensity for the specimen aged above 12 ksec was found to correspond to the crystallization of the MS-I phase. In fact, as the fluorescence term, $J_{fl}(s)$, did not change during the isothermal ageing, the changing part of SAXS intensity shown in Fig. 3 may be attributed to the change of $J_{coh}(s)$. The term $J_{fl}(s)$ could be evaluated as shown in Fig. 3, by summing up the scattering intensity from the constitutent pure elements multiplied by the respective molar fraction [26]. It was recognized that an appreciable value of $J_{coh}(s)$ is lying on the $J_{fl}(s)$ term for the as-quenched $Pd_{76}Au_6Si_{18}$. For further discussion, the $J_{coh}(s)$ term was transformed into the point beam intensity $I_{coh}(s)$ by using a computer program [20].

In the present study, the integrated intensity is defined by the equation,

$$\gamma(0) = \int_0^{s_{max}} 4\pi s^2 I_{coh}(s)\, ds \quad (2)$$

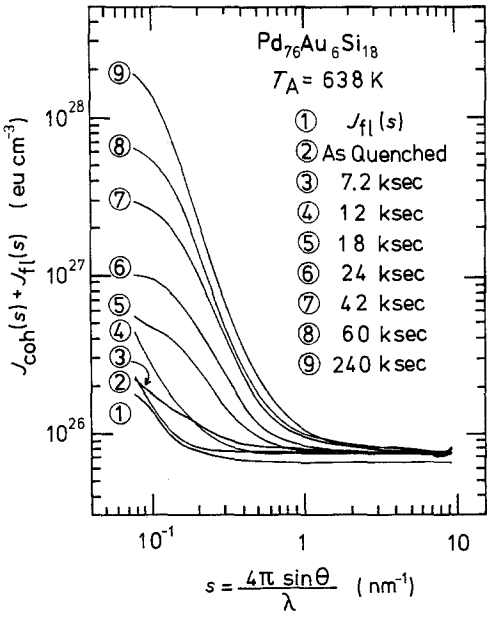

Figure 3 Change of SAXS intensity as a function of scattering vector for the amorphous $Pd_{76}Au_6Si_{18}$ alloys aged at 638 K, where $J_{fl}(s)$ is the fluorescence intensity and $J_{coh}(s)$ the intensity of coherent scattering.

where the upper limit was taken to be $s_{max} = 9.25\ nm^{-1}$. Fig. 4 shows the change of the integrated intensity during the isothermal ageing at various temperatures for the amorphous $Pd_{76}Au_6Si_{18}$ alloy. In the same figure, the time at which the crystalline phase was firstly detected by the large-angle diffraction measurement is also indicated. After the time indicated by MS-II, both MS-I and MS-II phase coexisted. It should be noted that the integrated intensity appears

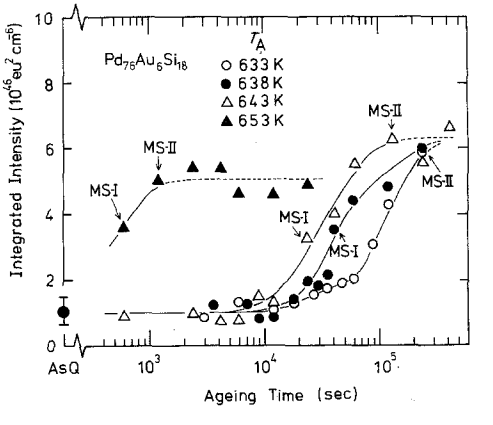

Figure 4 Dependence of the integrated intensity on ageing time. MS-I and MS-II show the time at which the crystalline phase was firstly detected by the large-angle diffraction measurements.

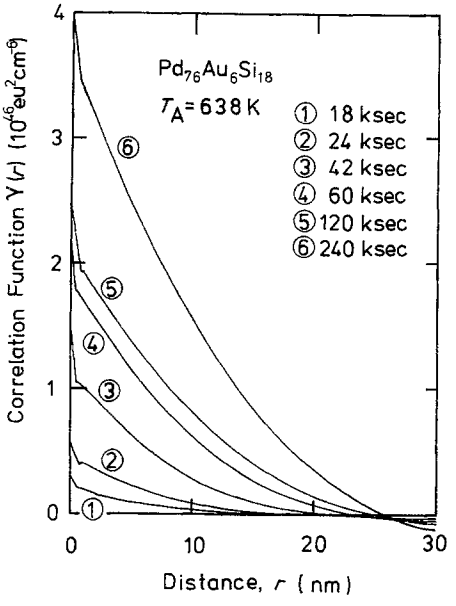

Figure 5 Density–density correlation function as a function of radial distance for the amorphous $Pd_{76}Au_6Si_{18}$ alloys aged at 638 K.

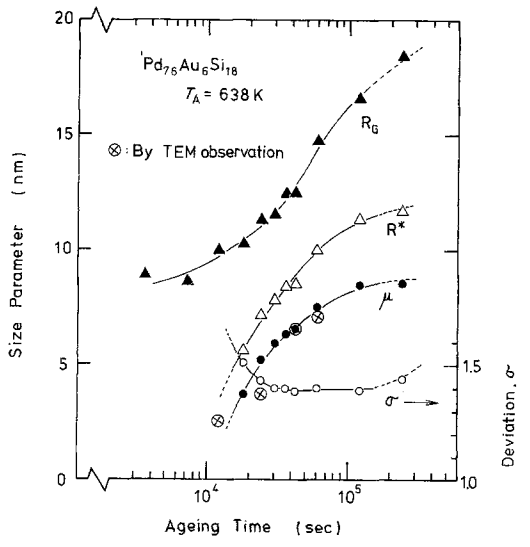

Figure 6 Ageing time dependence of size parameters for the amorphous $Pd_{76}Au_6Si_{18}$ alloys aged at 638 K, where R_G, R^*, μ and σ indicate Guinier radius, Porod radius, average radius in the log-normal size distribution and its deviation, respectively.

for the as-quenched specimen, even though its value was very small. When the specimen was aged below 643 K, the integrated intensity started to increase beyond ageing for times greater than 10 ksec. The higher the ageing temperature, the larger the integrated intensity. On the other hand, the ageing behaviour of the integrated intensity for the specimen aged at 653 K was different from the others. As its ageing temperature was near T_g, it was imagined that the transformation behaviour is transient in some places towards that in the supercooled liquid state, in which the diffusivity becomes very high compared with the diffusivity extrapolated from that below T_g [27].

The electron density–density correlation $\gamma(r)$ derived from the SAXS intensity [20] is shown in Fig. 5 for the specimens aged at 638 K. In general, the correlation decreased monotonically with increasing radial distance and become larger for the specimen aged for longer periods. Here the small hump appearing at the radial distance below 1 nm was concluded to be a result of the terminal effect in the Fourier integration. When the correlation is assumed to arise from an assembly of spherical particles with a size distribution, the expression is given by the equation [20],

$$\gamma(r) = N_p \Delta\rho^2 \langle V \rangle \left(1 - \frac{3r}{4R^*} + \frac{r^3}{16\langle R^3 \rangle}\right) \quad (3)$$

where N_p is the number density of particles, $\Delta\rho$ is the difference in electron density between the matrix and the particle, and $\langle V \rangle$ is the average volume of the particle. The size parameter R^* is called the Porod radius and can be obtained from the slope for the radial dependence of the correlation in the small region of radial distance.

It is unknown how those crystalline particles, as shown in Fig. 2, distribute in size. In the present study, the size distribution of those particles was assumed to obey the log-normal size distribution function [28],

$$F(r) = \frac{1}{2\pi^{1/2} r \ln\sigma} \exp\left[-\frac{1}{2}\left(\frac{\ln r - \ln\mu}{\ln\sigma}\right)^2\right] \quad (4)$$

where μ is the geometrical average and σ is the standard deviation. Both parameters can be determined experimentally by using the following relations [27],

$$\ln\mu = \ln R_G - \frac{12}{7}\ln\left(\frac{R_G}{R^*}\right) \quad (5)$$

$$\ln^2\sigma = \frac{2}{7}\ln\left(\frac{R_G}{R^*}\right) \quad (6)$$

where the size parameter R_G is called the Guinier radius, which can be obtained from the so-called Guinier plot of the SAXS intensity against scattering vector. Fig. 6 shows the change of these size parameters for the specimens aged at 638 K.

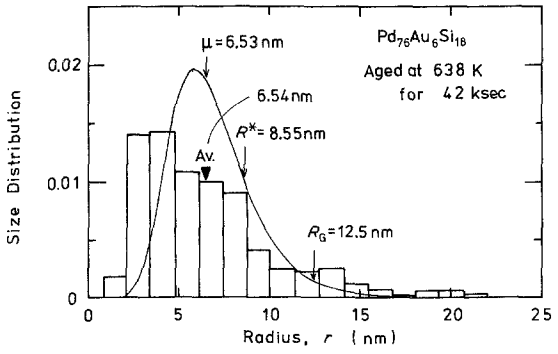

Figure 7 Histogram of the distribution of MS-I particles obtained by TEM observation for the amorphous $Pd_{76}Au_6Si_{18}$ alloy aged at 638 K for 42 ksec, where the log-normal size distribution determined by SAXS analysis is shown by the solid curve.

To check the appropriateness of the log-normal size distribution, the size distribution of particles was directly measured from the TEM photograph. Fig. 7 shows a comparison between both measurements of size distribution for the specimen aged at 638 K for 42 ksec. Histograms gave the results of counting the number in the interval of 1.33 nm from the TEM photograph, where the arithmetic average was 6.54 nm. The solid curve was calculated from Equation 4, after knowing both size parameters, R^* and R_G. It was found that the average size, $\mu = 6.53$ nm, was consistent with the arithmetic average determined from the TEM observation. Some of the arithmetic averages from TEM observations are plotted in Fig. 6.

Hereafter the log-normal size distribution was applied to express the structural features of the crystalline MS-I phase. Fig. 8 shows the change of size parameters during isothermal ageing for the specimens aged at various temperatures. The average radius, μ, increased with increasing ageing time and became larger for the specimens aged at the higher temperature. On the other hand, the standard deviation, σ, which indicates the measure of distribution in size,

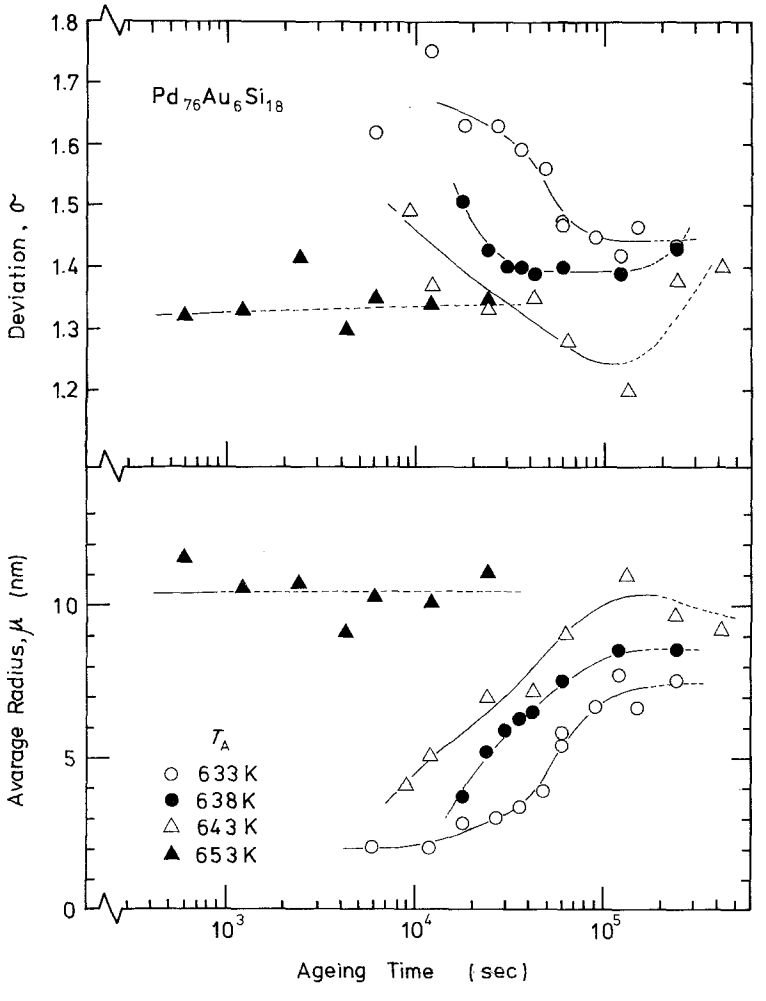

Figure 8 Ageing time dependence of size parameters in log-normal size distribution.

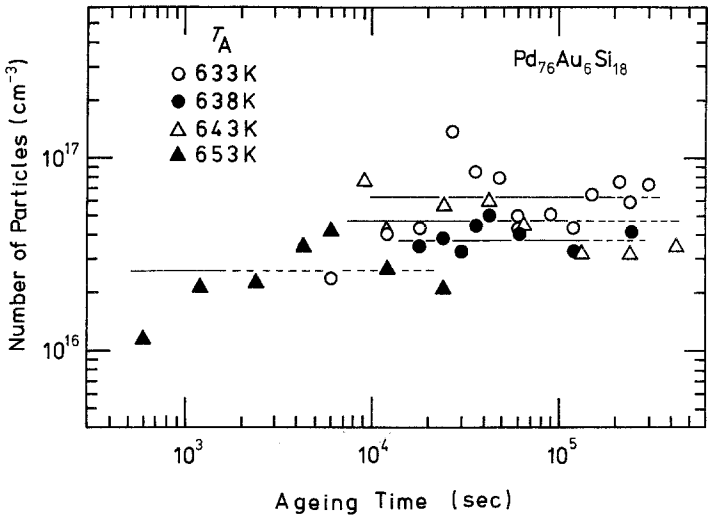

Figure 9 Ageing time dependence of number density of MS-I particles.

decreased with increasing ageing time and became smaller for the specimens aged at the higher temperatures. The number density of particles contributed to SAXS intensity was determined by using the relation discussed later. The result is shown in Fig. 9. The number density remained almost constant at the ageing conditions, after which the SAXS intensity increased remarkably. The number density attended to became larger for the specimens aged at the lower temperature.

4. Discussion

The present experimental results on the crystallization of the MS-I phase could be explained in the framework of the conventional nucleation theory as follows. As mentioned in Section 3, the lattice constant of the MS-I phase did not change during the isothermal ageing. This suggested that the composition of the MS-I phase was fixed as proposed to be $Pd_{78}Au_{22}$. The relative position of its composition is displayed in Fig. 10. When the tie line through the alloy composition is extrapolated to the opposite side, the terminal goes to Pd_3Si, which was just the MS-II phase. Therefore the decomposition process could be simply described as shown in Fig. 11, where the vertical axis is expressed in dimensions of electron density. When the MS-I phase with electron density of ρ_p crystallized, the electron density of the amorphous matrix, ρ_m, decreased apart from ρ_0, which is the value for the as-quenched specimen. During the further crystallization, the volume fraction, V_f of MS-I phase increased, but the electron density, ρ_m decreased and approached to the value of Pd_3Si. After the crystallization of the MS-I phase has fully developed the MS-II phase crystallized as mentioned in Fig. 4. When the atomic volume for the MS-II phase does not change before and after its crystal-

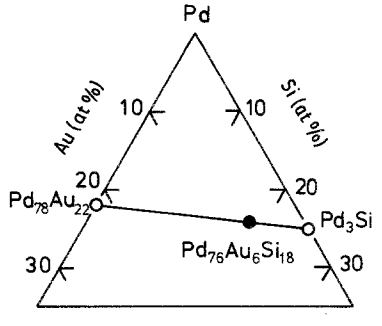

Figure 10 Locating of alloy composition in the Pd–Au–Si ternary diagram.

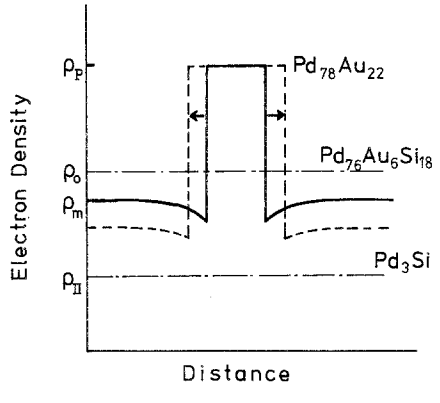

Figure 11 Schematic representation of the change of electron density partially crystallized specimen, in which the crystalline MS-I phase has a composition $Pd_{78}Au_{22}$.

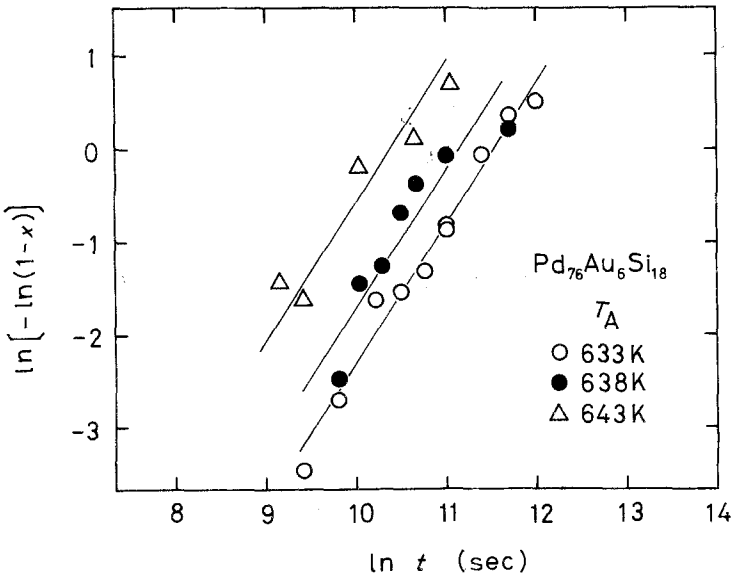

Figure 12 Johnson–Mehl–Avrami plots of the fraction transformed to the MS-I phase as a function of ageing time.

lization, the influence on SAXS intensity might be neglected as this situation could be recognized from Fig. 11.

In such a model for the inhomogeneous structure, the integrated intensity can be given by the correlation function at $r = 0$,

$$\gamma(0) = (\rho_p - \rho_m)^2 V_f(1 - V_f) \quad (7)$$

When the average atomic volume of the amorphous matrix was assumed not to change during the ageing in comparison with the initial value, the integrated intensity was reduced to the equation,

$$\gamma(0) = (\rho_p - \rho_m + \rho_p \frac{v_p - v_0}{v_0} V_f)^2 V_f/(1 - V_f) \quad (8)$$

where v_0 and v_p are the average atomic volume of the as-quenched specimen and the MS-I phase, respectively. Both values were experimentally determined as $v_0 = 0.0130\,\text{nm}^{-3}$ and $v_p = 0.0152\ \text{nm}^{-3}$, respectively. As shown typically in Fig. 7, the MS-I phase distributes in size. When the number of spherical particles with radius R is given by $n(R)$, the volume fraction of the MS-I phase is given by the equation,

$$V_f = \int_0^\infty \frac{4}{3}\pi R^3 n(R)\,dR = \frac{4}{3}\pi\langle R^3\rangle N_p \quad (9)$$

where the relation $n(R) = N_p F(R)$ was used and

$$\langle R^n\rangle = \int_0^\infty R^n F(R)\,dR \quad (10)$$

Fig. 9 shows the calculated results of N_p using Equation 9. When the volume fraction of the MS-I phase after completion of the phase separation is expressed by V_f^∞, the degree of transformation at a particular instant is given by the equation,

$$X(t) = \frac{V_f}{V_f^\infty} \quad (11)$$

According to the formal theory of precipitation kinetics [29], the fraction is expressed by

$$X(t) = 1 - \exp[-(t/\tau)^m] \quad (12)$$

The analytical result, by using the logarithmic manipulation of Equation 12, is shown in Fig. 12. The constant, m, was found to be in the range 1.38 to 1.48 which is nearly equal to 3/2. On the other hand, prior to the crystallization of MS-I, the structure relaxation was reported to occur in the present alloy [19]. From the analysis of DSC data, the exponent, m, has been determined to take a value of 0.5 during such a relaxation process [30]. The value 3/2 suggests that the present crystallization process is governed by the diffusion mechanism. In this case, the constant, τ, is given by the equation [29],

$$\tau = \left(\frac{2}{3}kN_p^{2/3}D\right)^{-1} \quad (13)$$

where

$$k = (48\pi^2 V_f^\infty)^{1/3} \quad (14)$$

and D is the interdiffusion constant. As shown in Fig. 4, the integrated intensity tended to saturate with the same magnitude for the three ageing conditions with different ageing temperatures,

TABLE I Analytical results of the relaxation time τ and interdiffusion constant D as a function of ageing temperature T_A

T_A(K)	τ (sec)	D (m^2 sec^{-1})
633	1.0×10^5	1.9×10^{-21}
638	6.9×10^4	3.7×10^{-21}
643	3.2×10^4	7.1×10^{-21}

so that V_f^∞ was put here as a constant. From the phase relation shown in Fig. 10, V_f^∞ was calculated to be 0.27. As the number density of particles has been determined as shown in Fig. 9, the diffusion constant was evaluated from Equation 13. The results are listed in Table I. The magnitude is of the order of 10^{-21} m^2 sec^{-1}, which is reasonable in comparison with the reported values of the interdiffusion constant for $Pd_{74}Au_8Si_{18}$ [14], and of the diffusion constant of palladium [12] and gold [27] in $Pd_{77.5}Cu_6Si_{16.5}$. The activation energy was obtained to be 420 kJ mol^{-1} from the present data, which agreed with 400 kJ mol^{-1} determined by the Kissinger method from DSC measurements [31].

Fig. 13 shows the change of size distribution of MS-I particles during the isothermal ageing at 638 K. It seems to be well represented that the size distribution diffuses out apparently along with increasing the average radius. In the present analysis it was thought that each particle grows according to the diffusion-controlled mechanism as soon as their size exceeds a critical size. Here an incubation time, t_i, is defined for the formation of critical nuclei with a nucleation flux of $K(t_i)$. The growth of each particle might be measured as a function of $(t_A - t_i)$, where t_A is the real time, that is, ageing time. In the early stage of transformation, when the fraction X is small, the time evolution of radius could be expressed as

$$R(t_A) = [2DV_f^\infty(t_A - t_i)]^{1/2} \quad (15)$$

where the size of the critical nucleus was assumed to be negligibly small. Now the function $K(t_i)$ can be estimated by using the size distribution after the ageing for the time t_A as shown in Fig. 13. Namely the particle with the size $R(t_A)$ at ageing time t_A was suggested to have nucleated at t_i according to Equation 15.

The nucleation flux at time t_i was assumed to be crudely proportional to the size distribution function, $F[R(t_A)]$. The result is shown in Fig. 14, where the parameters, D and V_f^∞ were used as described in the above paragraph. Significant results were as follows. The nucleation of the MS-I phase was mostly attained up to the ageing time of about 10 ksec at 638 K, especially the considerable amount of nuclei had already existed in the as-quenched specimen, even though no sign of nuclei and/or particles of MS-I phase could be observed by the present TEM technique.

Another possible mechanism to explain the structure change in the amorphous state could be the spinodal decomposition reported in the Pd–Au–Si alloy by Chou and Turnbull [14]. When this regime operated, one should observe an oscillation in the radical distance dependence of the electron density–density correlation reflecting the concentration waves. As seen in Fig. 5, any oscillatory component was not detected in the correlation, so that the spinodal decomposition was concluded not to occur within the present experimental conditions for the amorphous $Pd_{76}Au_6Si_{18}$ alloy. The observation of homogeneous distribution of MS-I particles

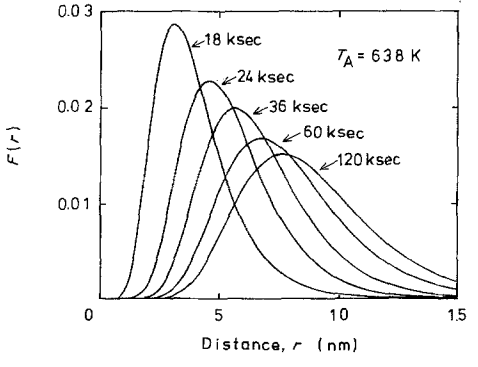

Figure 13 Calculated log-normal size distribution $F(r)$ for the specimens aged at 638 K for various times.

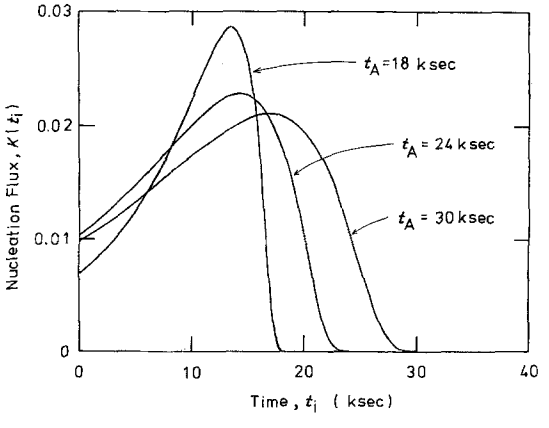

Figure 14 Time dependence of nucleation flux, $K(t_i)$, estimated from the size distribution.

without periodity, as shown in Fig. 2, might be thought to be circumstantial evidence for the present conclusion.

5. Conclusions

It was made clear that the crystallization of the amorphous $Pd_{76}Au_6Si_{18}$ alloy below T_g is accompanied by the phase separation into two phases, of which the major composition is $Pd_{78}Au_{22}$ and Pd_3Si, respectively, and the respective phase is crystallized as the MS-I and MS-II in sequence. The crystallization kinetics of the MS-I phase was quantitatively analysed by using mainly the SAXS data in the framework of the conventional nucleation theory. It was suggested that the considerable number of nuclei of the MS-I phase had been already formed in the as-quenched specimen and the remaining nucleation attained within the short period of isothermal ageing. The remarkable increase of SAXS intensity during the isothermal ageing corresponded to the growth of MS-I phase, where the number density of MS-I particles remained almost constant. The volume fraction of the crystallized MS-I phase was determined from the SAXS integrated intensity and the size distribution was found to be reasonably explained by using the log-normal size distribution function. The growth kinetics was concluded to be controlled by the diffusion mechanism. The evaluated values of diffusion data were in good agreement with the data reported by the other authors.

Acknowledgements

The authors would like to acknowledge many helpful discussions with Professor P. H. Shingu. They also thank Mr K. Shibue for his invaluable experimental work. Financial support for this work came partially from the Ministry of Education, Science and Culture under Research Contract No. 56211030, for which one of the authors (KO) wishes to express his gratitude.

References

1. P. DUWEZ, R. H. WILLENS and R. C. CREWDSON, *J. Appl. Phys.* **36** (1965) 2267.
2. B. G. LEWIS and H. A. DAVIES, *Mater. Sci. Eng.* **23** (1976) 179.
3. T. MASUMOTO and R. MADDIN, *Acta Metall.* **19** (1971) 725.
4. J. J. BURTON and R. RAY, *J. Non-Cryst. Solids* **6** (1971) 393.
5. P. DUHAJ, V. SLÁDEK and P. MRAFKO, *ibid.* **13** (1973/74) 341.
6. P. DUHAJ, D. BARANČOK and A. ONDREJKA, *ibid.* **21** (1976) 411.
7. N. FUNAKOSHI, T. KANAMORI and T. MANABE, *Jpn. J. Appl. Phys.* **17** (1978) 11.
8. K. TOKUMITSU, S. NANAO, H. INO and S. NISHIKAWA, *Trans. Jpn. Inst. Met.* **22** (1980) 210.
9. T. B. MASALSKI, Y. W. KIN, L. F. VASSAMILLET and R. W. HOPPER, *Mater. Sci. Eng.* **47** (1981) P1.
10. H. S. CHEN and D. TURNBULL, *Acta Metall.* **17** (1969) 1021.
11. B. G. BAGLEY and E. M. VOGEL, *J. Non-Cryst. Solids* **18** (1975) 29.
12. B. G. BOSWELL and G. A. CHADWICK, *Scripta Metall.* **10** (1976) 509.
13. N. FUNAKOSHI, T. KANAMORI and T. MANABE, *Jpn. J. Appl. Phys.* **16** (1977) 515.
14. C. -P. P. CHOU and D. TURNBULL, *J. Non-Cryst. Solids* **17** (1975) 169.
15. J. SITEK, M. PREJSA, J. CIRÁK, M. HUCL and J. LIPKA, *ibid.* **28** (1978) 225.
16. H. INO, S. NANAO and T. MUTO, *J. Phys. Soc. Jpn.* **46** (1979) 63.
17. K. USTUMI and K. KAWAMURA, *Trans. Jpn. Inst. Met.* **21** (1980) 269.
18. M. MARCUS, *J. Non-Cryst. Solids* **30** (1979) 317.
19. R. SUZUKI, K. SHIBUE, K. OSAMURA, P. H. SHINGU and Y. MURAKAMI, *J. Mater. Sci. Lett.* **1** (1982) 127.
20. K. OSAMURA and Y. MURAKAMI, *J. Jpn. Inst. Met.* **43** (1979) 537.
21. J. B. NELSON and D. P. RILEY, *Proc. Phys. Soc. Lond.* **57** (1945) 160.
22. A. MAELAND and T. B. FLANAGAN, *Canad. J. Phys.* **42** (1964) 2364.
23. M. HANSEN and K. ANDERKO, "Constitution of Binary Alloys" (McGraw-Hill Book Co., New York, 1958) 1125.
24. JCPDS card No. 17–369.
25. K. OSAMURA, K. SHIBUE, R. SUZUKI and Y. MURAKAMI, *Colloid and Polymer Sci.* **259** (1981) 677.
26. K. OSAMURA, R. SUZUKI and Y. MURAKAMI, in "Proceedings of the 4th International Conference on Rapidly Quenched Metals" Vol. 1 Sendai, August 1981, edited by T. Masumoto and K. Suzuki (Japan Institute of Metals, Sendai, 1982) p. 431.
27. H. S. CHEN, L. C. KIMERLING, J. M. POATE and W. L. BROWN, *Appl. Phys. Lett.* **32** (1978) 461.
28. M. E. FINE, "Introduction to Phase Transformations in Condenced Systems" (The Macmillan Company, New York, 1965) p. 53.
29. S. D. HARNESS, R. W. GOULD and J. J. HREN, *Phil. Mag.* **19** (1969) 115.
30. R. O. SUZUKI and P. H. SHINGU, in "Proceedings of the 5th International Conference on Liquis and Amorphous Metals", Los Angeles, August 1983, in press.
31. R. O. SUZUKI and P. H. SHINGU, to be published.

Received 28 July
and accepted 12 September 1983